# MODELLING THE EFFECTS OF FABRIC STRUCTURE ON THE VARIABILITY OF PERMEABILITY

C.C. Wong, A.C. Long [1] and C.D. Rudd

*School of Mechanical, Materials and Manufacturing Engineering,*
*University of Nottingham, University Park, Nottingham, NG7 2RD, U.K.*

[1] Corresponding author's email: andrew.long@nottingham.ac.uk

**ABSTRACT:** Textile permeability in general shows a high variance. This work describes a method to model textile variability at the meso-scopic scale based on a generalised textile model. Inhomogeneities were introduced into the textile structure by randomly moving the tow paths at the crossovers according to a given Normal distribution. The effects of textile structure on the evaluated permeability variations were explored and demonstrated using non-crimp fabric and plain weave models. Fabric architecture was shown to be important in that it imposed a limit to the degree of variations of the tows. This study demonstrated that significant insights in flow behaviour for textile reinforcements can be provided by an efficient 2D model.

**KEYWORDS:** Liquid Composite Moulding (LCM), textile permeability, numerical simulation, variability.

## INTRODUCTION

One of the crucial phases in Liquid Composite Moulding (LCM) processes is the injection of resin into the mould cavity. Impregnation of the textile reinforcement is determined by the textile permeability, which is a measure of the ease of fluid flow. In general, textile permeability shows a high variation [1, 2], consequently affecting the quality and cycle time of the product. This makes it difficult to predict the filling pattern and fill times accurately, thus reducing productivity.

Several researchers have studied the various factors which would affect fabric permeability values. Pan et al. [3] performed controlled uni-directional flow experiments for a plain weave and a 0°/90° non-crimp glass fibre fabric, and found that the permeability of the fabrics was primarily influenced by local changes in fibre deformation and superficial fabric density. Hoes et al. [4] measured the distributions of permeability for a plain weave, twill weave and a special PVC-coated layered fabric, using a radial flow method. They used the latter material to show that nesting is the major source of the variations in permeability values. The permeability scatter for all the fabrics tested in both studies was found to follow a Normal distribution.

In order to study the influence of fabric structure on permeability, Endruweit et al. [5] analysed five fabrics with different architecture and geometrical parameters and measured permeability using a radial flow set-up with automated data collection and analysis. They concluded that the more homogeneous the structure of a material, the lower is the permeability variation. In an attempt to model the variations observed experimentally, Endruweit et al. [6] assumed that the variation in local permeability is primarily caused by stochastic variations in fibre spacing, from which local permeability values can be calculated.

Injection simulations at the component level were then simulated for a bi-directional non-crimp fabric for a range of variations in fibre spacing to determine the global permeability variations. A trend was found between relative permeability variations and the maximum frequency of fibre tow waviness, which agreed with the experimental values. In general, the global permeability variation decreased with increasing mould dimensions.

The above attempted to describe the variations at the macro-scopic level. It is equally important to address variability at the meso-scopic level. Essentially, a fabric is defined by its structure and the interaction between the fibre bundles is the key to the variability of the fabric. Only by looking at the meso-scopic level can one analyse the effect of fabric architecture on variability and address issues such as localised inhomogeneities.

Using optical microscopy and X-ray micro-computed tomography, Desplentere et al. [7] measured geometrical parameters of the fibre bundles in 3D textiles. Considerable variations were found for these geometrical dimensions. Lundstrom et al. [8] determined the local permeability of non-crimp fabrics (NCF) from the dimensions of the flow channels with variable widths between the fibre tows. For a completely random distribution of the local permeability values, the global permeability was found to decrease with increasing maximum variation at the unit cell level, while for a correlated distribution, the permeability can either increase or decrease. To further study the effect of geometry variations on local permeability, Nordlund and Lundstrom [9] modelled the meso-scopic channels of a non-crimp fabric with variations in width, height and shape of the channels and the effect of the presence of stitches. The study identified the geometrical parameters that have the greatest affect on the local permeability. In order to realistically predict flow for a NCF, the effects of the stitching process and statistical variations of the channel dimensions have to be included in the model.

This study attempts to address permeability variation by modelling variability in the meso-scopic structure of the fabric itself. Specifically, the effect of fabric architecture on the variability of permeability is analysed. In contrast to the works of Lundstrom et al. [8] and Nordlund and Lunstrom [9], which are specific to NCFs, the methodology here is based on using a generalised textile modeller, TexGen [10]. Variability is modelled by randomly disturbing the paths of the fibre bundles according to a statistical distribution, and the effective permeability of the randomised flow domain is calculated based on a numerical method known as Grid Average [11].

## MESO-SCALE PERMEABILITY MODELLING METHODS

### TexGen

Textile models are generated using an in-house textile schema, TexGen [10]. It begins with vectors defining the textile interlacing pattern, which are smoothed and have volumes created around them to represent the tows. An analysis domain is defined in which the tows are repeated accordingly to fill up the domain. Some useful built-in functions include slice extraction, in-plane shearing to represent the effects of draping and statistical tow paths randomisation to emulate the variability seen in textiles (as described below). Output options include input files to mesh generators (for FE or CFD analyses) and data files for in-house permeability models, e.g. Grid Average [11] as used here.

### Grid Average method

The Grid Average method [11] was developed to reduce the complexity of the flow problem. Firstly, the flow domain is discretised into a regular square grid in the x-y plane, as shown in Figure 1. For each grid element, the local permeability tensor is calculated as the thickness-weighted average of the individual permeabilities of the respective layers contained within the element. The permeability of a free channel with height $h$ is approximated to $h^2/12$ (from laminar flow between paallel plates) and the permeability of the porous tow is specified based on the fibre volume fraction using simple analytical models from Gebart [12], whereby the tows are modelled locally as either quadratic or hexagonal arrays of unidirectional fibres.

Periodic boundary conditions are imposed on the four sides of the computational domain. A pressure difference, $\Delta P$, is imposed in a direction parallel to one of the global axes. Darcy's Law is coupled with the continuity equation to derive a partial differential equation for fluid pressure, which is then solved for saturated flow based on a finite difference scheme. The resulting flow rate is calculated from the evaluated pressure field, from which the effective permeability of the domain in the flow direction is back calculated using Darcy's Law.

**Tow variations**

In TexGen, variability in textile models is generated using the Monte-Carlo method, whereby the tow crossovers points within the fabric are randomly displaced along the global x- and y-axes independently. This movement will follow a Normal distribution with respect to the original coordinates of the points and a user-specified standard deviation of displacement. As the tow movement variation is increased, the tows will invariably begin to interfere with one another. In this study, cases with tow interference are discarded. The actual tow position distribution can be easily back calculated for a set of randomised cases.

The randomised model is dicretised using the Grid Average method. As periodic boundary conditions are imposed on the four sides of the flow domain in the solution, it is imperative that the model itself exhibits periodicity. For the analysis of a unit cell as shown in Figure 1, only two basic tows representing each layer are needed to ensure periodicity, with lengths equivalent to the diagonal dimension of the domain. A unit cell is defined here as the domain with the minimum dimensions which forms a repeatable representative cell of the fabric.

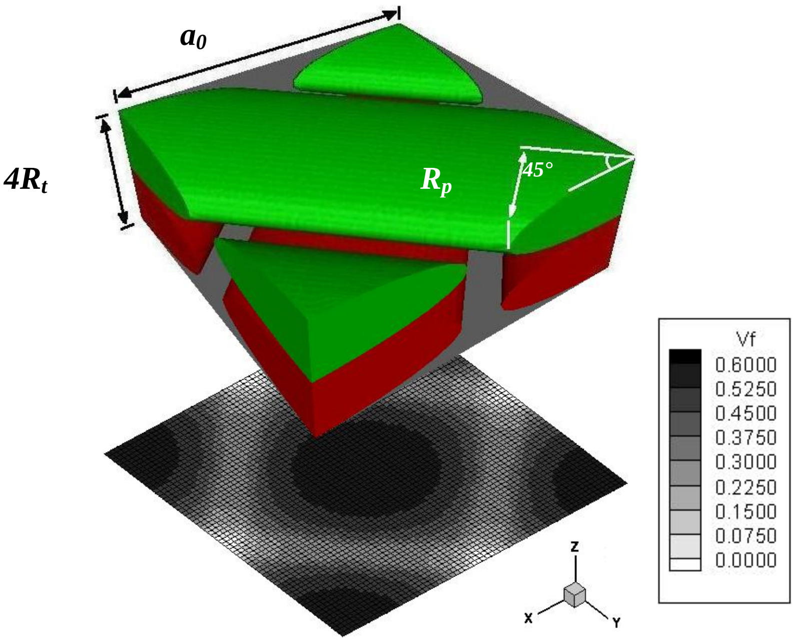


Figure 1 - Unit cell of a ± 45° non-crimp fabric model with dimensions as shown (top) and the discretised Grid Average mesh showing fibre volume fraction (bottom).

## RESULTS

A plain weave and a non-crimp fabric (NCF) are modelled here (see Figure 2). Both the models have elliptical tow cross sections with semi major axis, $R_p$ = 0.7mm and semi minor axis, $R_t$ = 0.175mm, $a_0$ = 2.6mm and no stitches present in the NCF model (see Figure 1 for definition of dimensions). The upper and lower layers of these models are not touching, so that tow variations can be introduced in the plain weave without resulting in interference. The tow local permeability is calculated for 60% $V_f$ based on the Gebart model for a quadratic array of fibres. The computational domain size is 2.6 x 2.6 x 0.85mm, with nominal cell fibre volume fractions of 29.3% and 30.6% for the NCF and plain weave models respectively. The models are discretised using 50 divisions per unit, resulting in Grid Average meshes containing 17161 nodes. A pressure difference of $10^5$ Pa is imposed in the direction of the global x-axis with a resin viscosity $\eta$ of 0.308 Pa s (although permeability is independent of these values).

Randomised cases were generated for the two models by applying two standard deviations of nodal displacement at 14.83% and 29.65% with respect to the spacing between the tows. For each model and different tow variations, a total of 100 randomised cases were simulated and evaluated statistically. The achieved levels of tow variability and resultant mean and standard deviations of $V_f$, $\alpha$ and $K_x$ are listed in Table 1. Generally, the standard deviation of $K_x$ increases with increasing tow variations. Interestingly, the mean value of $K_x$ for the NCF model decreased with increasing variability whilst the mean $K_x$ value for the plain weave increased slightly.

The degree of permeability variation is somewhat limited for the plain weave cases. For the NCF model, when the tow position variation is doubled, there is an increase in permeability variations from 1.24% to 4.18%. The plain weave model exhibited an increase of only 11% in permeability variations from 1.73% to 1.93%. Similar observations can be made on the relative increase in the variations of the fibre volume fraction and fibre angle. The standard deviation of the fibre angles for the plain weave is almost the same for the two levels of tow path variability.

At applied tow movement variations of 14.83% and 29.65%, the NCF cases achieved variations of 10.50% and 20.83% respectively whilst the plain weave cases achieved 8.69% and 13.12% respectively. The plain weave model has reached its geometric limit of variation at an applied variation of 29.65%, as evident from the low level of resultant variability of 13.12%. In fact, 7 out of 10 randomised plain weave cases with 29.65% tow variation had to be discarded because of tow interference. The plain weave structure restricts the mobility of the tows more than the NCF does, and this is reflected in the permeability variation.

a) b)

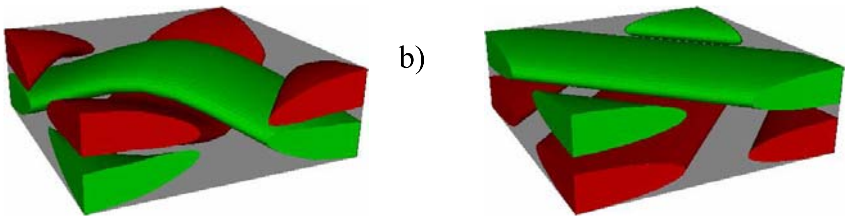

Figure 2 - (a) Plain weave model with $a_0$ = 2.6mm, $R_p$ = 0.7mm and $R_t$ = 0.175mm and (b) corresponding NCF model. Note the gap between the layers in both models.

Table 1 - Mean and standard deviation values for a NCF and a plain weave model with $a_0$ = 2.6mm, $R_p$ = 0.7mm and $R_t$ = 0.175mm.

| **Std. dev. of nodal position as % wrt space between tows** | | **$V_f$** | **α (deg)** | **$K_x$ (x $10^{-9}$ $m^2$)** |
|---|---|---|---|---|
| **Intended** | **Achieved** | | | |
| **Bi-directional NCF** | | | | |
| 0.00 | 0.00 | 0.293 | 90 | 5.485 |
| 14.83 | 10.50 | 0.293 ± 0.000 (± 0.12%) | 89.99 ± 3.90 (± 0.04%) | 5.473 ± 0.068 (± 1.24%) |
| 29.65 | 20.83 | 0.294 ± 0.001 (± 0.41%) | 90.12 ± 6.93 (± 0.08%) | 5.347 ± 0.224 (± 4.18%) |
| **Plain weave** | | | | |
| 0.00 | 0.00 | 0.306 | 90 | 1.629 |
| 14.83 | 8.69 | 0.304 ± 0.000 (± 0.09%) | 89.98 ± 3.44 (± 0.04%) | 1.665 ± 0.029 (± 1.73%) |
| 29.65 | 13.12 | 0.305 ± 0.001 (± 0.21%) | 89.98 ± 4.47 (± 0.05%) | 1.674 ± 0.032 (± 1.93%) |

The permeability distribution the plain weave correlates better with a Normal distribution than for the NCF (see Figure 3). The plain weave structure restricts the movement of the tows, particularly at the tow crossover points, where the point of overlap cannot differ too much between randomised cases. Hence most of the randomised cases exhibited a similar pattern of variation, and the predicted pressure distributions were very close to one another (see Figure 4). Calculated permeability values are hence equally likely to lie on either side of the mean. In contrast, tows in the NCF are less restricted compared to the plain weave, exhibiting a wider range of possible variation patterns. For the NCF model, in extreme cases a whole tow can move closer to an adjacent tow, which is not possible for a plain weave where crossovers impose periodic restrictions. As a result, NCF models exhibit distorted and non-uniform pressure distributions, as shown in Figure 5. The calculated permeability values of these extreme cases are much lower than the nominal value, and this is reflected in the predicted permeability distribution for NCFs.

The observation here on the effect of fabric structure on the shape of the permeability distribution is interesting, implying that fabric structure has an important influence on permeability variations at the meso-scale. However, published experimental observations [4, 5] suggest that the Normal distribution of permeability is seen for most types of fabrics. One can argue that as the NCF model used here does not include stitches as seen in a real NCF, then the tows are freer to move, creating more variable patterns. A previous study [13] has also indicated that it is perhaps more appropriate to model a larger domain when variability is involved.

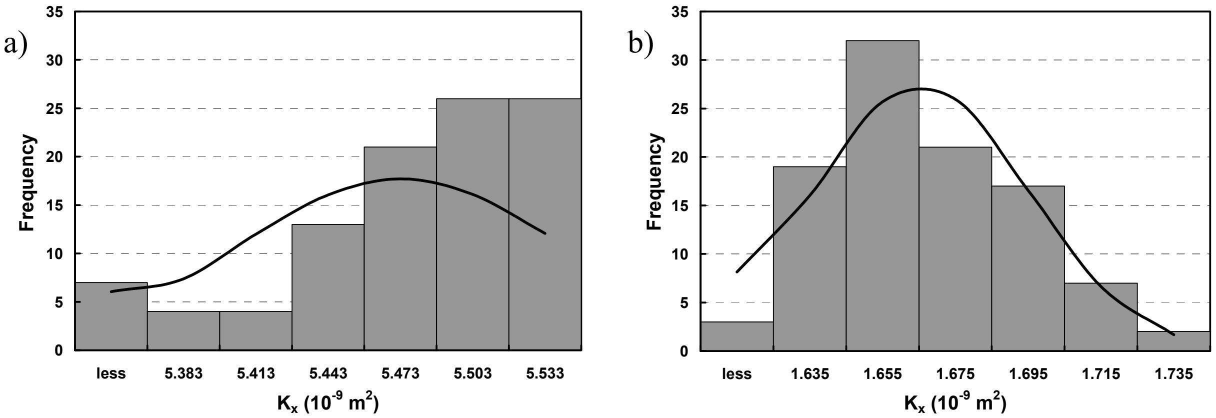


Figure 3 - Distributions of predicted $K_x$ for (a) NCF and (b) plain weave models with applied nodal displacement standard deviation of 14.83% with respect to the spacing between the tows. Corresponding Normal distributions are shown with correlation coefficients of 0.648 and 0.934 respectively.

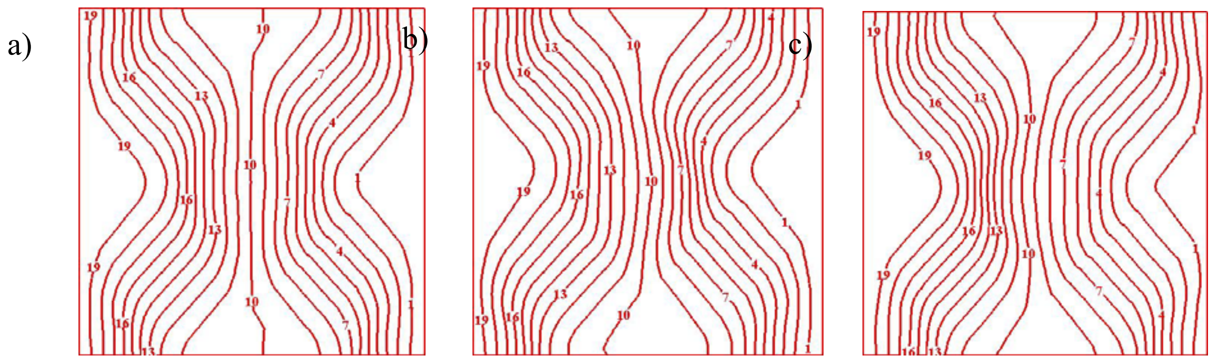


Figure 4 - Pressure distributions of (a) the nominal plain weave model with no tow variability and (b & c) typical cases with extreme tow variability. (a) The nominal case exhibits symmetrical pressure contours about the centre line 10. The pressure distributions in (b) and (c) are still quite similar to that of the nominal case (a).

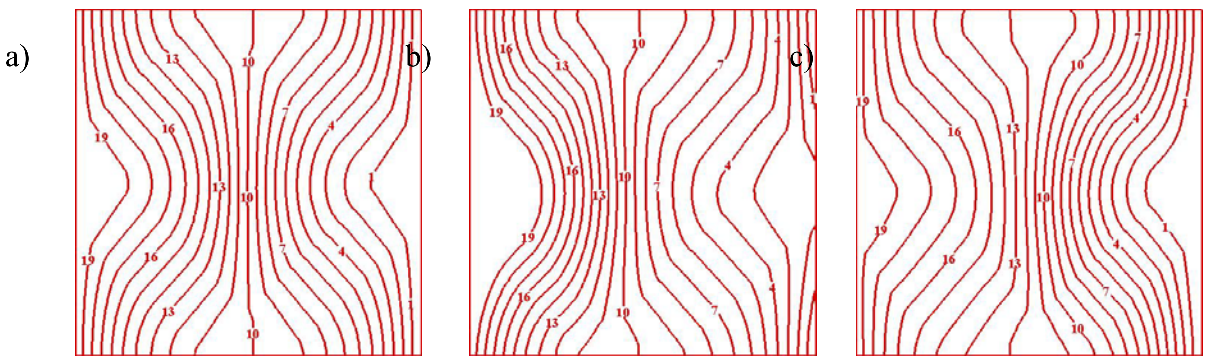


Figure 5 - Pressure distributions of (a) the nominal NCF model with no tow variability and (b & c) typical cases with extreme tow variability. (a) The nominal case exhibits symmetrical pressure contours about the centre line 10. In (b), the pressure distribution is distorted compared to (a) whereas in (c), the pressure contours are not symmetrical as line 10 has shifted to the right.

## DISCUSSION

This study addresses variability in permeability at the meso-scopic scale. In this respect it is fundamentally different to previous studies which have addressed macro-scopic variability [3-6]. For example Endruweit's variability model [6] is applicable to a macro-scopic flow simulation where the effect of the structure is rather homogenised. The meso-scopic models presented here are based purely on the fabric architecture which is useful to address issues such as localised inhomogeneities. This may allow local phenomena such as a void formation to be studied in detail.

One limitation of the present study is that the fabric models have idealised geometries with a low fibre volume fraction, i.e. a lot of free space between the tows. The effective permeability of the domain will be dominated by the free space permeability, which is several orders of magnitude higher than the tow permeability, and thus variations of the tow paths will be less important. Furthermore, experimental measurements are based on several layers of fabric and nesting will affect the variability of permeability as shown in [4].

There are various ways to model variability in the textile models. In this study, the tows are assumed to move randomly at the crossover points according to a Normal distribution, which does not necessarily happen in real life. Non-crimp fabrics have stitches running through them, which would influence the tow alignment. Furthermore, the fibre tows, being long and tortuous, would be less likely to be randomly displaced at each crossover.

## CONCLUSIONS

Textile permeability in general shows a high variation. Consequently, researchers have attempted to model such variability in order to better predict the filling times and flow pattern of LCM processes. This paper has described a method to model textile variability at the meso-scopic scale based on a generalised textile modeller. Inhomogeneities were introduced into the textile structure by randomly moving the tow paths at the crossovers according to a Normal distribution.

The variations of permeability for a plain weave fabric were compared to a NCF model with a similar cell fibre volume fraction. The architecture of the fabric is important in that it imposes a limit to the degree of variations of the tow paths. From the comparison between two types of fabric, the plain weave was seen to restrict the movement of the tows more than the NCF. This has two effects: the permeability variation is lower for the plain weave and the permeability distribution correlates better with a Normal distribution. This study demonstrated that significant insights in flow behaviour for textile reinforcements can be provided by an efficient 2D model.

## ACKNOWLEDGEMENTS

The authors would like to acknowledge Martin Sherburn and Francois Robitaille for developing some of the theories and software that made the studies in this paper possible. The support of the following organisations is also acknowledged: UK Engineering and Physical Sciences Research Council (EPSRC), Dowty Propellers (Smiths Aerospace), ESI Software, Ford Motor Company and Formax UK Ltd.

## REFERENCES

1. Lundstrom, T.S., R. Stenberg, R. Bergstrom, H. Partanen, and P.A. Birkeland, *In-plane permeability measurements: a nordic round-robin study.* Composites Part A, 2000. **31**(1): p. 29-43.
2. Luo, Y., I. Verpoest, K. Hoes, M. Vanheule, H. Sol, and A. Cardon, *Permeability measurement of textile reinforcements with several test fluids.* Composites Part A, 2001. **32**(11): p. 1497-1504.
3. Pan, R., Z. Liang, C. Zhang, and B. Wang, *Statistical characterizaton of fiber permeability for composite manufacturing.* Polymer Composites, 2000. **21**(6): p. 996-1006.
4. Hoes, K., D. Dinescu, H. Sol, R.S. Parnas, and S. Lomov, *Study of nesting induced scatter of permeability values in layered reinforcement fabrics.* Composites Part A, 2004. **35**: p. 1407-1418.
5. Endruweit, A., P. McGregor, A.C. Long, and M.S. Johnson, *Influence of the fabric architecture on the variations in experimentally determined in-plane permeability values.* Composites Science and Technology, 2005. Accepted for publication.
6. Endruweit, A. and A.C. Long, *Influence of stochastic variations in the fibre spacing on the permeability of bi-directional textile fabrics.* Composites Part A, 2005. **37**(5): p. 679-694.
7. Desplentere, F., S.V. Lomov, D.L. Woerdeman, I. Verpoest, M. Wevers, and A. Bogdanovich, *Micro-CT characterization of variability in 3D textile architecture.* Composites Science and Technology, 2005. **65**(13): p. 1920-1930.
8. Lundstrom, T.S., V. Frishfelds, and A. Jakovics, *A statistical approach to permeability of clustered fibre reinforcements.* Journal of Composite Materials, 2004. **38**(13): p. 1137-1149.
9. Nordlund, M. and T.S. Lundstrom, *Numerical Study of the Local Permeability of Noncrimp Fabrics.* Journal of Composite Materials, 2005. **39**(10): p. 929-947.
10. Sherburn, M., F. Robitaille, A. Long, and C. Rudd. *Geometric pre-processor for the calculation of physical properties of textiles*. in *Industrial Simulation Conference*. 7-9 June 2004. University of Malaga, Spain: EUROSIS-ETI.
11. Wong, C.C., A.C. Long, M. Sherburn, F. Robitaille, P. Harrison, and C.D. Rudd, *Comparisons of novel and efficient approaches for permeability prediction based on the fabric architecture.* Composites Part A, 2006. **37**(6): p. 847-857.
12. Gebart, B.R., *Permeability of unidirectional reinforcements for RTM.* Journal of Composite Materials, 1992. **26**(8): p. 1100-1133.
13. Wong, C.C. and Long, A.C, *Modelling variations of textile fabric permeability at the meso-scopic scale*. Accepted for publication in Plastics, Rubber and Composites.